arXiv:cond-mat/0210145v3 [cond-mat.supr-con] 12 Sep 2003

Evidence for Nodal Quasiparticles in the Non-magnetic Superconductor YNi_2B_2C via Field-angle-dependent Heat Capacity

Tuson Park and M. B. Salamon

Department of Physics and Material Research Laboratory, University of Illinois at Urbana-Champaign, IL 61801, USA

Eun Mi Choi, Heon Jung Kim, and Sung-Ik Lee

National Creative Research Initiative Center for Superconductivity and Department of Physics, Pohang University of Science and Technology, Pohang 790-784, Republic of Korea

(Dated: Dec 24, 2002)

Abstract

Field-angle dependent heat capacity of the non-magnetic borocarbide superconductor YNi_2B_2C reveals a clear fourfold oscillation, the first observation of its kind. The observed angular variations were analyzed as a function of magnetic field angle, field intensity and temperature to provide its origin. The quantitative agreement between experiment and theory strongly suggests that we are directly observing nodal quasiparticles generated along $< 100 >$ by the Doppler effect. The results demonstrate that field-angle heat capacity can be a powerful tool in probing the momentum-space gap structure in unconventional superconductors such as high T_c cuprates, heavy fermion superconductors, etc.

Most superconductors behave "conventionally;" electronic excitations are suppressed by the BCS energy gap causing the electronic heat capacity, for example, to be exponentially small at temperatures well below the superconducting transition. Recently, a number of superconductors, cuprates and heavy-fermion metals among them, have been found to be "unconventional" in that they exhibit gap-zero (or nodal) points or lines in momentum space. Electronic excitations–nodal quasiparticles (nqp)–are then observed at low temperatures, giving rise to power-law rather than exponential, behavior. Unlike gapless superconductivity, which can occur in conventional superconductors, the Fermi momenta of these quasiparticles are restricted to nodal regions of the Fermi surface, giving a strong directional dependence to various physical properties. While pioneering work by Salamon and coworkers [1, 2] and by subsequent experimenters [3, 4] demonstrated the directionality of thermally excited nqp's via the thermal conductivity, direct detection has proven elusive.

The rare earth borocarbide superconductors RNi_2B_2C (R=Y, Lu, Tm, Er, Ho, and Dy) had been generally thought to exhibit isotropic s-wave pairing via electron-phonon coupling [5, 6, 7, 8, 9], but there is growing evidence that the gap function is highly anisotropic or has a nodal structure on the momentum surface [4, 10, 11, 12, 13, 14]. In specific heat measurements, a power law behavior was observed in the temperature dependence and the electronic coefficient $\gamma(H)$, to the extent it can be extracted, follows a square-root field dependence [10, 15]. Low temperature thermal conductivity measurements showed low energy excitations that also indicate unconventional superconductivity [11]. Recently, Izawa and coworkers reported a field-directional-angle dependence of the thermal conductivity in YNi_2B_2C that suggested point nodes along $< 100 >$ directions [4]. However, their interpretation is not definitive because the highly anisotropic nature of the Fermi surface and nonlocality could lead to anisotropic macroscopic phenomena even within the ab-plane [16]. Angular specific heat measurements, however, are insensitive to the Fermi surface topology and reflect the gap anisotropy through the Doppler energy shift [17]. We report here the first observation of Doppler-induced angular dependence of the electronic heat capacity in the non-magnetic borocarbide superconductor YNi_2B_2C.

In order to study the elusive angular variation in the low temperature specific heat [18, 19], we built a probe specifically designed to look at the DOS variation with field angle. The probe was designed to fit into a Quantum Design Physical Properties Measurement System with a 7 T transverse magnet. The heat capacity of YNi_2B_2C was measured by ac calorimetry

in which the sample was heated by an electronically modulated laser pulse and the induced ac temperature was measured by chromel-gold/iron (0.07%) thermocouple. In order to account for the magnetic field dependence of the thermocouple wire, the ac signal from a non-magnetic dummy sample was measured vs magnetic field in the temperature range of interest. As the heat capacity is field independent, any change with field arises from the thermocouple wire and was used to correct the data. The details of the ac technique can be found elsewhere [20].

The single crystal YNi_2B_2C was grown by the high temperature flux method using Ni_2B as a solvent. The details are described elsewhere [21, 22]. The inset of the Fig. 1 shows the superconducting transition at 0 T. The sharp thermodynamic transition ($\Delta T/T_c \leq 0.02$) indicates that the sample is homogeneous.

The main graph of Fig. 1 shows the field dependence of the heat capacity at 2.5 K. The sample was zero-field cooled to 2.5 K and a magnetic field was applied along the (100) direction. The open circles describe the heat capacity with increasing field and the crosses, with decreasing field. There is a deviation between the two below 1 T, which indicates that flux pinning is important at low magnetic fields. The system enters into the normal state above 5.2 T along this direction and the lower critical field is less than 0.1 T. The heat capacity with increasing magnetic field was fitted by $C_0 + b\ (H - H_0)^{1/2}$ (**dashed line**). The excellent square-root fit up to the upper critical field indicates that YNi_2B_2C is a superconductor with an unconventional pairing symmetry. In an intermediate field range, $H_{c1} \ll H \ll H_{c2}$, the square root field dependence comes mostly from nqp's induced by the Doppler effect; the core-state contribution becomes important as the field approaches H_{c2} [15, 23].

The upper panel of Fig. 2 shows the field-directional angular dependence of the total heat capacity at 2 K in 1 T. The field angle α was measured with respect to the a-axis. The transverse magnetic field was rotated within the basal plane of YNi_2B_2C by increments of 3° by a computer controlled stepping motor. Repositioning the sample by 33° relative to the thermocouples and apparatus shifts the 4-fold pattern, but not the 2-fold contribution, by that angle. The total heat capacity consists of constant, 2-fold, and 4-fold contributions: $C_{total}(\alpha) = C_0 + C_2(\alpha) + C_4(\alpha)$. The field-independent constant C_0 is due to nonmagnetic contributions such as the lattice heat capacity and thermally excited nqp's, and is determined experimentally in C vs H data. The 2-fold contribution $C_2(\alpha)$ comes from our experimental

setup and has a functional form of $c_2 \cos 2\alpha$. The Au/Fe thermocouple wire is a major source of this contribution but misalignment of the basal plane of the sample against the field direction could also lead to the 2-fold component because of the anisotropy between in-field ab-plane and c-axis heat capacities. The dashed line in the upper panel of the Fig. 2 is $C_2(\alpha)$; the 2-fold signal is about 48 % of the 4-fold component at 1 T and increases with magnetic field up to 55 % at 4 T. The circles in the lower panel of the Fig. 2 describe the 4-fold part $C_4(\alpha)$, which clearly reveals the angular variation.

In the mixed state of an unconventional superconductor, the supercurrent flows around a vortex lead to a Doppler energy shift, $\delta\omega \sim \mathbf{v}_s \cdot \mathbf{k}_F$, where $\mathbf{v}_s$ is the velocity of the superfluid and $\mathbf{k}_F$ is the Fermi momentum of nodal quasiparticles. When the field direction is normal to the plane containing nodes, the DOS is the average over the whole Fermi surface, leading to a square-root field dependence [15]. When the field is in the nodal plane, however, the Doppler shift has a field-direction dependence as well, $\delta\omega \approx \frac{E_h}{\rho} \sin\beta \sin(\phi - \alpha)$ [17]. Here ϕ is an azimuthal angle of the gap node and β is a vortex current winding angle. $\mathrm{E}_h = \frac{a\hbar v_F}{2}\sqrt{\pi H/\Phi_0}$ is the energy scale associated with the Doppler effect. The geometrical constant a is order of unity, v_F is the Fermi velocity, and Φ_0 is the flux quantum. The variable $\rho = r/R$, where r is the distance from the vortex core and $2R$ is the intervortex distance. Working in the 2D limit, Vekhter *et.al.* calculated the DOS , $N \approx (N_1 + N_2)/2$, for an in-plane magnetic field when $\omega, E_h \ll \Delta_0$ and for four nodes at angles α_n from orthogonal axes in a plane :

$$\frac{N_i(\omega, h, \alpha)}{N_0} = \begin{cases} \frac{\omega}{\Delta_0}(1 + \frac{1}{2x^2}) & (x = \omega/E_i \geq 1) \\ \frac{E_i}{\pi\Delta_0 x}[(1 + 2x^2)\arcsin x + 3x\sqrt{1 - x^2}] & (x \leq 1), \end{cases} \quad (1)$$

where i = 1,2, $E_1 = E_h|\sin(\alpha_n - \alpha)|$ and $E_2 = E_h|\cos(\alpha_n - \alpha)|$. N_0 is the normal-state density of states. The directional dependence of the Doppler effect, therefore, leads to the oscillation of the DOS where it has minima along nodes and maxima along antinodes. At T = 0 K, the oscillation is cusped with a contrast of $1/\sqrt{2}$ between the minima and the maxima and is independent of the magnetic field. At a finite temperature, however, the sharp contrast is washed out and the DOS oscillation now depends on the magnetic field.

As seen in Fig. 2, our data are well described by the cusped function $|\sin 2\alpha|$ which will be used in the analysis of the 4-fold variation. To make a quantitative analysis, we fit our data to $C_4(h, \alpha) = c_4(1 + \Gamma|\sin 2\alpha|)$. The coefficient c_4 and the angular contrast Γ were treated as field dependent fitting parameters. The solid line in the lower panel of Fig. 2 shows the fit with $\Gamma = 0.05$ in 1 T. The sharp minima along $< 100 >$ indicate that there

exist gap minima or nodal structures along those directions. That the nodal positions are at $< 100 >$ is consistent with the angular thermal conductivity measurement [4].

The contrast Γ depends on the gap geometry and dimensionality of the superconductor. The Vekhter et al. model above assumes the Fermi momentum of nqp's to be restricted to the nodal plane. Recent band calculations show that YNi_2B_2C has a 3D electronic structure in spite of its layered structure [6]. A more realistic calculation, therefore, is to allow nqp Fermi momentum out of the nodal planes, which decreases the amplitude of the angular variation. Following Won et al. [24], we use a modulated cylindrical Fermi surface and account for the 3D effect by replacing the Doppler related energies E_1 and E_2 by $E_1^{3D} = E_h[\sin^2(\alpha_n - \alpha) + \cos^2\theta]^{1/2}$ and $E_2^{3D} = E_h[\cos^2(\alpha_n - \alpha) + \cos^2\theta]^{1/2}$ respectively and integrate the DOS over polar angle θ:

$$N(w, h, \alpha) = \frac{1}{2\pi}\int_0^{2\pi}\frac{1}{2}[N_1(w, h, \alpha, \theta) + N_2(w, h, \alpha, \theta)]d\theta. \quad (2)$$

The heat capacity ratio, $C(2K, h, \alpha)/C(2K, h, 0)$, calculated from the DOS, is displayed as a 3D surface vs magnetic field-angle α (x-axis) and H (y-axis) in Fig. 3(a). In Fig. 3(b), we show the experimentally obtained data sets after subtraction of the background contributions. Since the in-plane oscillation is due only to the Doppler effect, $C_4(2K, h, \alpha)/C_4(2K, h, 0)$ corresponds to the theory. We used 0.6, 1, 1.5, and 2 T data sets to construct the contour both in numerical and experimental plots. The Doppler energy scale E_h was adjusted to get a best fit, giving the Fermi velocity of $v_F = \sqrt{v_a v_c} = 1.3 \times 10^7$ cm/s which is comparable to other reported values [25]. We used the geometrical constant $a = 1$ and $\Delta = 1.76 k_B T_c$. Note that the angle contrast between experiment and theory are in good agreement suggesting that we are directly observing Doppler-shift generated nqp's. The periodicity of the peaks is $\pi/2$ and the oscillations grow with increasing field because of the increased Doppler energy.

Fig. 4 compares the contrast between node and antinode, $\Gamma(2K, h) = [C(2K, h, \pi/4) - C(2K, h, 0)]/C(2K, h, 0)$ from experiment (**open circles**) with numerical values (**dashed line**). Above $h = 0.5$, the data deviates from the theoretical prediction. One source of deviation is the Zeeman energy splitting μH, where μ is Bohr magneton, discussed recently by Whelan and Carbotte [26]. At a critical field H_c, Zeeman and Doppler energy scales become comparable and the DOS variation with field angle vanishes. It is unlikely, however, that the deviation comes from the effect because the

critical field is $\sim 10^2$ T. A more likely possibility is that the deviation is evidence that the core-state contribution to the electronic specific heat becomes significant in the high field regime. When we include the core states, the parameter C_4 consists of the core and the nodal contributions : $C_4(\alpha) = C_{core} + C_{node}(\alpha)$. Since the oscillation anisotropy Γ measures the amplitude of the 4-fold pattern against the nodal part only, we need to subtract the core part from the C_4, resulting in an increased anisotropy in our data. In order for a quantitative analysis, it is essential to distinguish the contributions from the core states and the extended states.

The inset of the Fig. 4 shows the contrast Γ vs temperature in 1 T. The basal plane of the sample was misaligned by 26° from the field direction, which produced a larger 2-fold contribution as was expected due to the heat capacity anisotropy between ab-plane and c-axis. The temperature dependence of the anisotropy was compared with the 3D nqp model that was used in the above analysis. The dashed line is the estimated anisotropy with the same Doppler energy scale with $v_F = 1.3 \times 10^7$ cm/sec. It explains the temperature dependence of the oscillation amplitude very well, corroborating that the nodal quasiparticles are Doppler shifted.

Before concluding this report, we want to discuss the possible pairing symmetries of YNi_2B_2C. Observation of the four-fold angular variation in our heat capacity measurement limits the candidates to those with gap minima or nodes with singlet pairing states such as anisotropic s-wave, d-wave or mixtures of two or more order parameters. Recently, Izawa et al. reported a clear fourfold pattern in the c-axis thermal conductivity at 0.27 K, which sets the gap-anisotropy ratio to be much higher than 100 [4]. One can still argue for gap minima, but a more natural explanation will be the presence of nodes in momentum space. We note that the field-angle heat capacity will have 4-fold pattern for both d-wave and anisotropic s-wave gap with nodes. Considering the significance of the pairing symmetry to understand the superconductivity in YNi_2B_2C and further to understand the interplay of magnetism and superconductivity in RNi_2B_2C (R = Tm, Er, Ho, and Dy), other measurements such as phase sensitive π junction SQUID or tunneling measurements are required to distinguish those anisotropic order parameters

In summary, we have reported the first direct evidence for a variation of the density of states of nodal quasiparticles due to a field-induced Doppler energy shift through a four-fold field-angle oscillation in the heat capacity. The angular variation, together with the

$\sqrt{H}$ variation of the heat capacity at 2.5 K, strongly suggests that the gap function is extremely anisotropic or, more likely, that YNi_2B_2C is an unconventional superconductor. The magnetic field-angle, field-intensity and temperature dependence of the heat capacity are in quantitative agreement with a model in which the fourfold pattern arises from Doppler-enhanced, fully 3D nodal quasiparticles with momenta in $< 100 >$ directions.

This project was supported in part by NSF Grant No. DMR 99-72087 and at Pohang by the Ministry of Science and Technology of Korea through the Creative Research Initiative Program. X-ray measurements were carried out in the Center for Microanalysis of Materials, University of Illinois, which is partially supported by the U.S Department of Energy under grant DEFG02-91-ER45439. We thank H. Yanagihara and C. D. Benson for help in building the probe. T. Park thanks N. Goldenfeld for stimulating comments and discussions.

---

[1] M. B. Salamon, F. Yu, and V. N. Kopylov, J. Supercon. **8**, 449 (1995).

[2] F. Yu, M. B. Salamon, and A. J. Leggett, Phys. Rev. Lett. **74**, 5136 (1995).

[3] H. Aubin, K. Behnia, and M. Ribault, Phys. Rev. Lett. **78**, 2624 (1997).

[4] K. Izawa, K. Kamata, Y. Nakajima, Y. Matsuda, and T. Watanabe, Phys. Rev. Lett. **89**, 137006 (2002).

[5] S. A. Carter, Phys. Rev. B **50**, 4216 (1994).

[6] L. F. Mattheis, Phys. Rev. B **49**, 13279 (1994).

[7] H. Michor, T. Holubar, C. Dusek, and G. Hilscher, Phys. Rev. B **52**, 16165 (1995).

[8] R. Gonnelli, A. Morello, G. A. Ummarino, V. A. Stepanov, G. Behr, G. Graw, S. V. Shulga, and S. L. Drechsler, Int. J. Mod. Phys. B **14**, 2840 (2000).

[9] S. Manolo and E. Schachinger, J. Low Temp. Phys. **123**, 149 (2001).

[10] M. Nohara, M. Isshiki, H. Takagi, and R. J. Cava, J. Phys. Soc. Jpn. **66**, 1888 (1997).

[11] E. Boaknin, R. W. Hill, C. Proust, C. Lupien, and L. Taillefer, Phys. Rev. Lett. **87**, 237001 (2001).

[12] I.-S. Yang, M. V. Klein, S. L. Cooper, P. C. Canfield, B. K. Cho, and S.-I. Lee, Phys. Rev. B **62**, 1291 (2000).

[13] K. Izawa, A. Shibata, Y. Matsuda, Y. Kato, H. Takeya, K. Hirata, C. J. van der Beek, and M. Konczykowski, Phys. Rev. Lett. **86**, 1327 (2001).

[14] K. Maki, P. Thalmeier, and H. Won, Phys. Rev. B **65**, 140502 (2002).

[15] G. E. Volovik, JETP Lett. **58**, 469 (1993).

[16] V. Metlushko, U. Welp, A. Koshelev, I. Aranson, and G. W. Crabtree, Phys. Rev. Lett. **79**, 1738 (1997).

[17] I. Vekhter, P. J. Hirschfeld, J. P. Carbotte, and E. J. Nicol, Phys. Rev. B **59**, R9023 (1999).

[18] K. A. Moler, D. J. Baar, J. S. Urbach, R. Liang, W. N. Hardy, and A. Kapitulnik, Phys. Rev. Lett. **73**, 2744 (1994).

[19] Y. Wang, B. Revaz, A. Erb, and A. Junod, Phys. Rev. B **63**, 094508 (2001).

[20] T. Park, M. B. Salamon, C. U. Jung, M.-S. Park, K. Kim, and S.-I. Lee, Phys. Rev. B **66**, 134515 (2002).

[21] B. K. Cho, P. C. Canfield, L. L. Miller, D. C. Johnston, W. P. Beyermann, and A. Yatskar, Phys. Rev. B **52**, 3684 (1995).

[22] M.-O. Mun, S.-I. Lee, W. C. Lee, P. C. Canfield, B. K. Cho, and D. C. Johnston, Phys. Rev. Lett. **76**, 2790 (1996).

[23] M. Ichioka, A. Hasegawa, and K. Machida, Phys. Rev. B **59**, 184 (1999).

[24] H. Won and K. Maki, Europhys. Lett. **56**, 729 (2001).

[25] V. G. Kogan, M. Bullock, B. Harmon, P. Miranovic, L. Dobrosavljevic-Grujic, P. L. Gammel, and D. J. Bishop, Phys. Rev. B **55**, R8693 (1997).

[26] N. D. Whelan and J. P. Carbotte, Phys. Rev. B **62**, 14511 (2000).

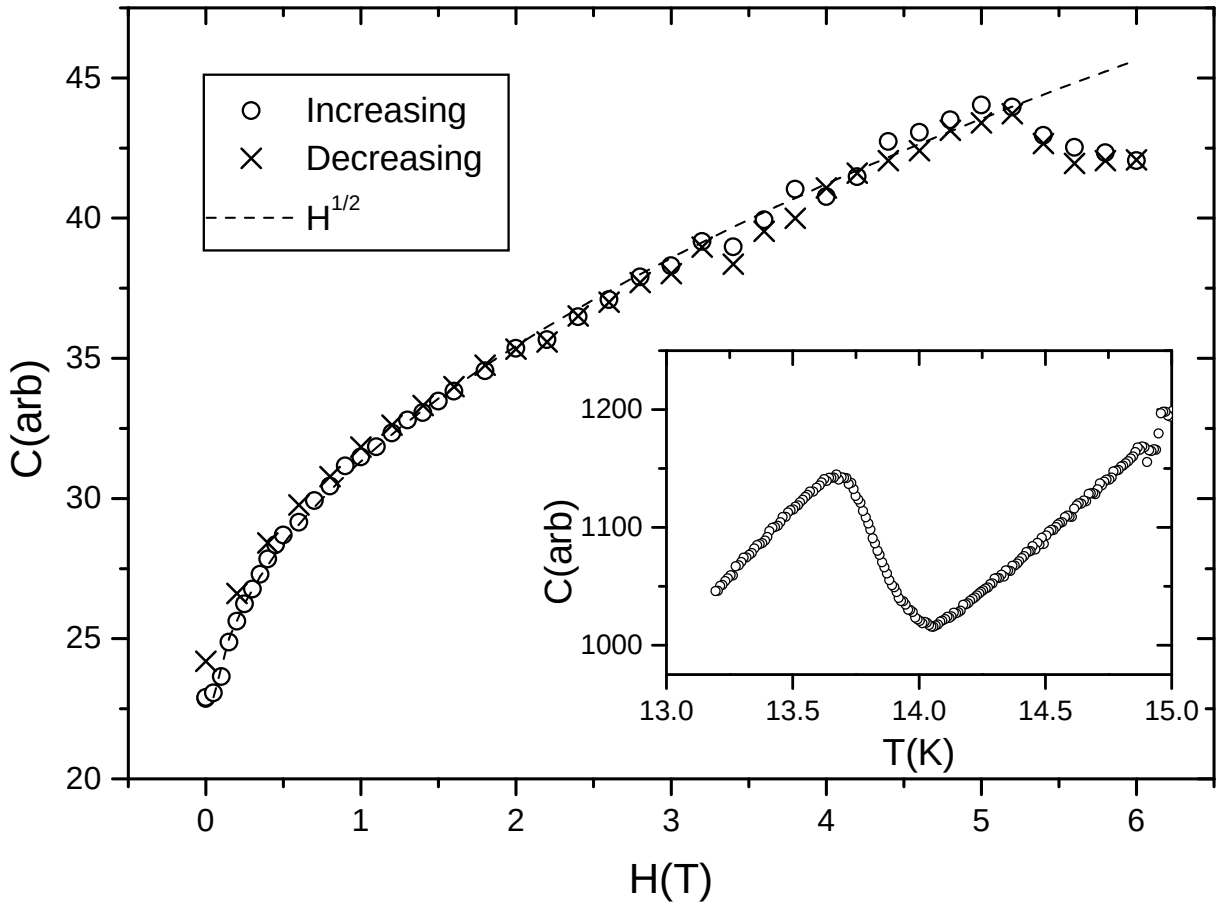


FIG. 1: Field dependence of the specific heat at 2.5 K along (100) direction. The open circles are with increasing magnetic field and the cross are with decreasing field. The dashed line describes $C_0 + b(H - H_0)^{1/2}$ with $C_0 = 23$, $b = 10$. H_0 is essentially due to Meissner effect and 0.09 T is used in the fit. The inset is the temperature dependence of the heat capacity around superconducting temperature at zero field.

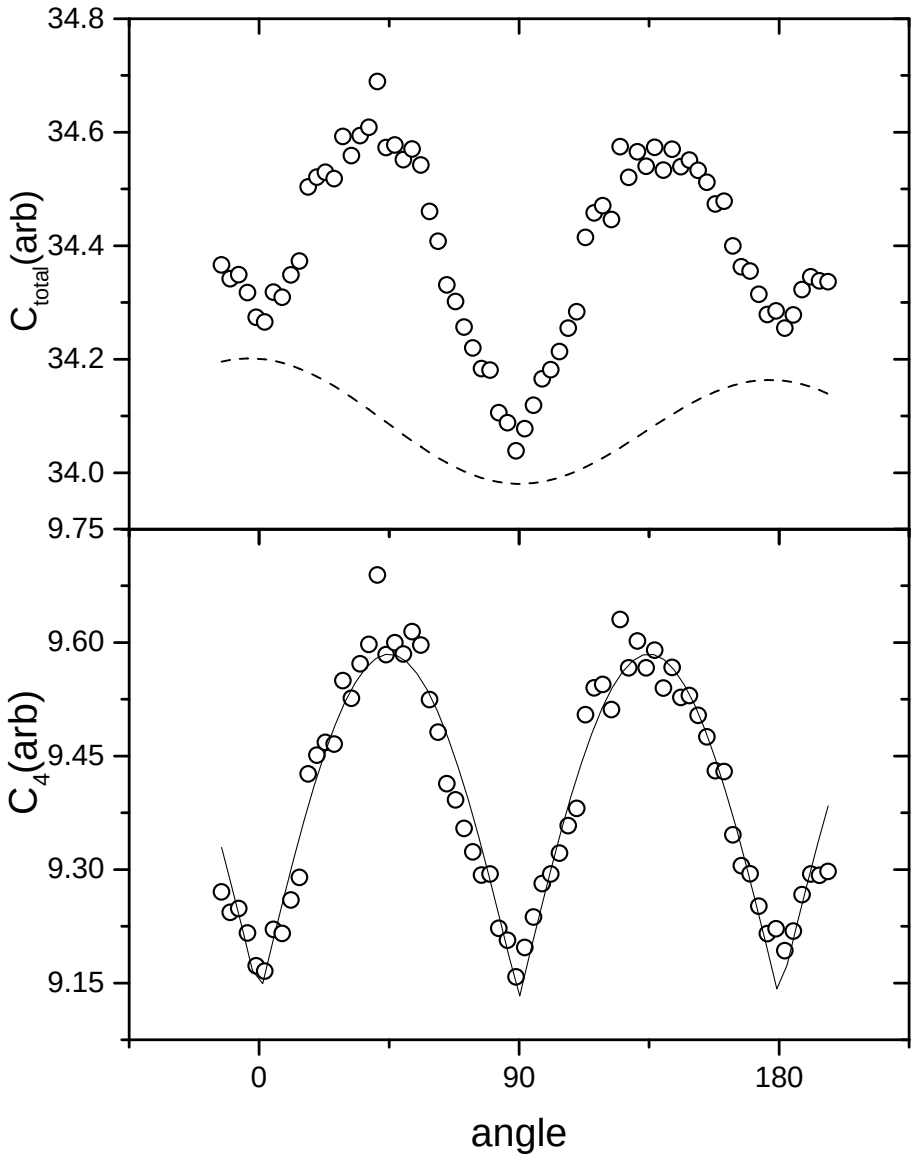


FIG. 2: Field directional dependence of the heat capacity at 2 K in 1 T. The field angle α is measured with respect to the a-axis. The top panel shows the total heat capacity (open circles) and the 2-fold component, $C_2(\alpha)$ relative to baseline of 34.1 (dashed line). The bottom panel shows the same data after subtracting the background, $C_4(\alpha) = C_{total}(\alpha) - C_0 - C_2(\alpha)$. The solid line describes a fit with a cusped function, $C_4(\alpha) = c_4(1 + \Gamma|\sin 2\alpha|)$ with $\Gamma = 0.05$.

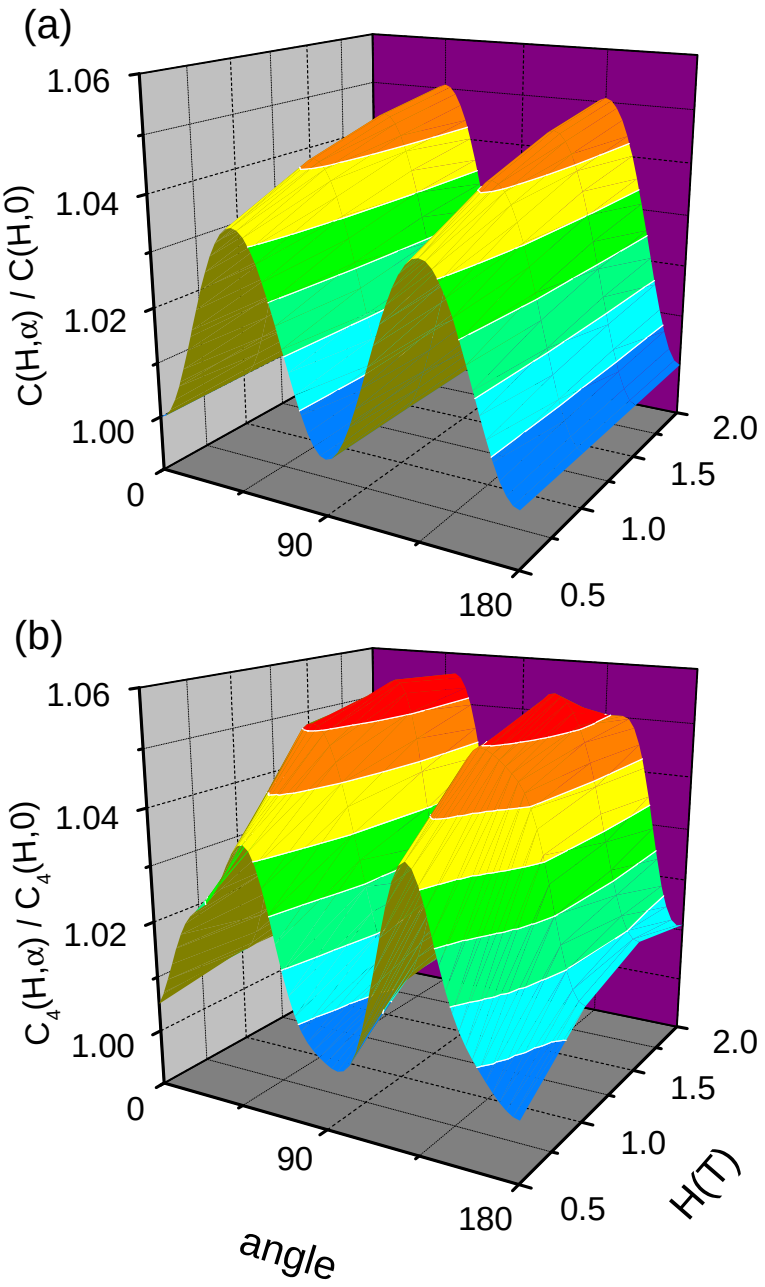


FIG. 3: The 3D surface plots describe magnetic field-angle (x-axis) and field-intensity (y-axis) dependence of the in-plane specific heat ratio at 2 K: $C(h,\alpha)/C(h,0)$. Fig. (a) is a numerical calculation of the specific heat due to nodal quasiparticles in 3D system and Fig. (b) is experimental data taken at 2 K in vortex phase. The experimental data were FFT low-pass filtered with a cut-off frequency of 0.03Hz with angles being considered as time. Both plots (a) and (b) were constructed with 0.6, 1, 1.5, 2 T data sets.

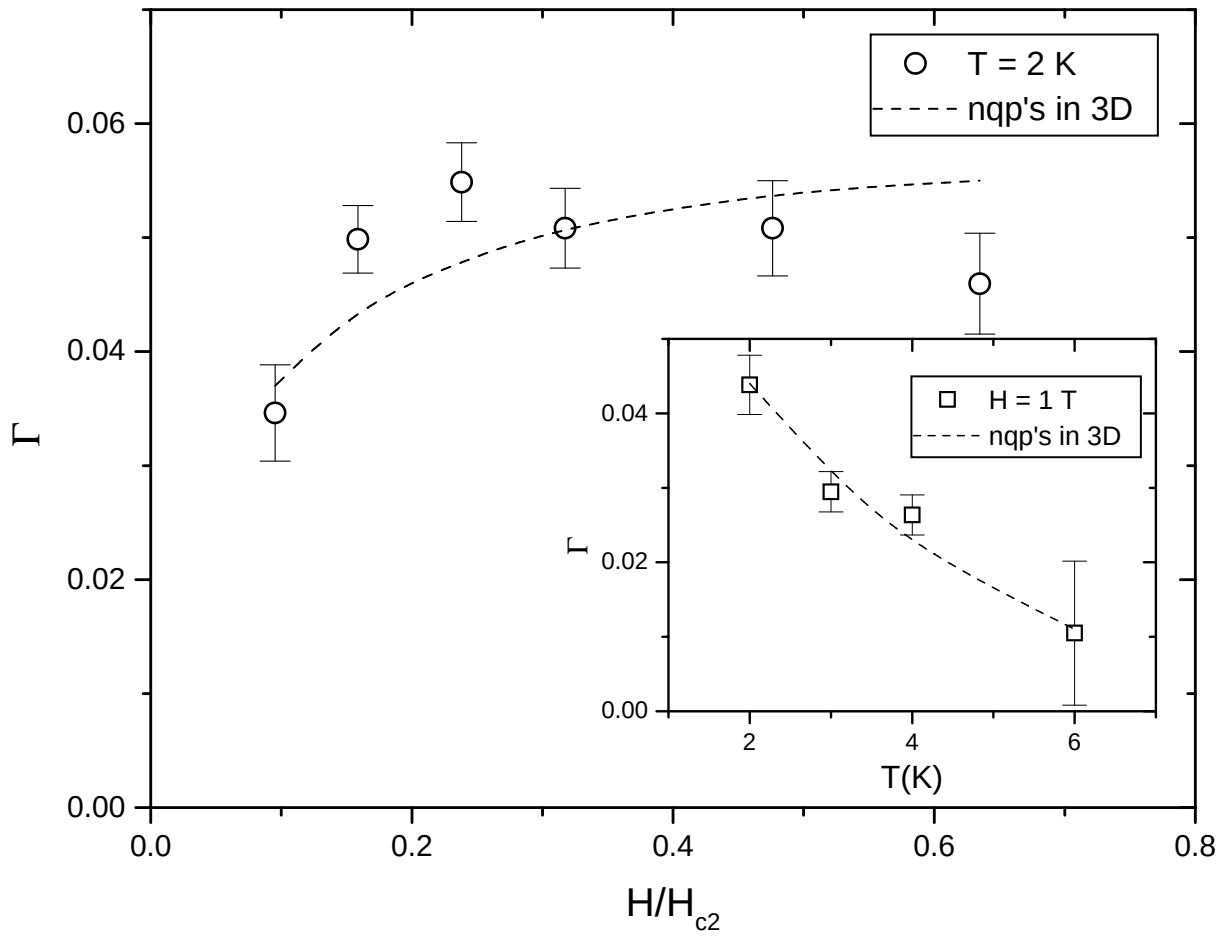


FIG. 4: The oscillation amplitude Γ at $\theta = 90^\circ$ is shown against the reduced field, H/H_{c2} at 2 K where H_{c2} is 6.3 T. The dashed lines in the main graph and in the inset are numerical estimations of the angular contrast by nqp's in 3D with the Fermi velocity $v_F = 1.3 \times 10^7$ cm/sec. Inset: The oscillation amplitude was shown against temperature in 1 T.